

# Performance Analysis of Cooperative Communications at Road Intersections Using Stochastic Geometry Tools

Baha Eddine Youcef Belmekki<sup>1,2</sup>, Abdelkrim Hamza<sup>1</sup>, and Benoît Escrig<sup>2</sup>

<sup>1</sup>LISIC Laboratory, Electronic and Computer Faculty, USTHB, Algiers, Algeria,  
email: {bbelmekki, ahamza}@usthb.dz

<sup>2</sup>University of Toulouse, IRIT Laboratory, School of ENSEEIHT, Institut National Polytechnique de Toulouse, France, e-mail: {bahaeddine.belmekki, benoit.escrig}@enseeiht.fr

## Abstract

Vehicular safety communications (VSC) are known to provide relevant contributions to avoid congestions and prevent road accidents, and more particularly at road intersections since these areas are more prone to accidents. In this context, one of the main impairments that affect the performance of VSC are interference. In this paper, we develop a tractable framework to model cooperative transmissions in presence of interference for VSC at intersections. We use tools from stochastic geometry, and model interferer vehicles locations as a Poisson point process. First, we calculate the outage probability (OP) for a direct transmission when the received node can be anywhere on the plan. Then, we analyze the OP performance of a cooperative transmission scheme. The analysis takes into account two dimensions: the decoding strategy at the receiver, and the vehicles mobility. We derive the optimal relay position, from analytical and simulation results, for different traffic densities and for different vehicles mobility models. We also show that the OP does not improve after the number of infrastructure relays reached a threshold value. Finally, we show that the OP performance of VSC is higher at intersections than on highways. We validated our analytical results by Monte-Carlo simulations.

## Index Terms

Cooperative communications, interference, outage probability, decode-and-forward, stochastic geometry, Poisson point process, vehicle-to-vehicle (V2V), vehicle-to-infrastructure (V2I), intersection.

## I. INTRODUCTION

### *A-Motivation:*

Road traffic safety is a major issue, especially at road intersections. Studies showed that 50% of all crashes are in junction roads (intersections) including fatal crashes, injury crashes and property damage crashes [1]. This makes intersections critical areas not only for vehicles, but also for cyclists and pedestrians. Vehicular communications offer a wide range of applications to avoid potential accidents, or to warn vehicles of an accident happening in their vicinity. Vehicular communications consist of vehicle-to-vehicle (V2V) communications, and vehicle-to-infrastructure (V2I) communications, in which vehicles interact with infrastructures, e.g. road-side units (RSUs). However, the main limiting factors that can jeopardize V2V and V2I communications, and degrade the performance in terms of outage probability are the interference originated from other transmitting vehicles [2]. Hence, understanding interference dependence is crucial when designing safety and low latency applications and protocols [3]. In order to deal with interference, cooperative communications have been shown to reduce the outage probability, and increase the throughput in the presence of interference [4].

### *B-Related works:*

Several works focus on the effect of interference using tools from stochastic geometry, and point process theory. However, few researches focus on interference dependence between interferer nodes and how it affects the performance considering direct transmissions [5]–[9], and cooperative transmissions (see [10]–[12] and references therein).

As far as V2V and V2I communications are concerned, several works investigated the effect of interference in highway scenarios [13]–[15]. In [16], the authors derive the expressions for the intensity of concurrent transmitters and packet success probability in multi-lane highways with CSMA MAC protocols. The performance of IEEE 802.11p using tools from queuing theory and stochastic geometry is analyzed in [17]. The outage probability is obtained in [18] for Nakagami-m fading and Rayleigh fading channels and the results are verified with real-world dataset containing the locations of Beijing taxis. The authors in [19] derive the outage probability and rate coverage probability of vehicles, when the line of sight path to the base station is obstructed by large vehicles sharing other highway lanes. In [20], the performance of automotive radar is evaluated in terms of expected signal-to-noise ratio, when the locations of vehicles follow a Poisson point process and a Bernoulli lattice process.

However, few works studied the effect of interference in vehicular communications at intersections. Steinmetz et al derive the success probability when the received node and the interferer nodes are aligned on the road [21]. In [22], the authors analyze the performance in terms of success probability for finite road segments under several channel conditions. The authors in [23] evaluate the average and the fine-grained reliability for interference-limited V2V communications with the use of the Meta distribution. In [24], the authors analyze the performance of an orthogonal street system which consists of multiple intersections, and show that, in high-reliability regime, the orthogonal street system behaves like a 1-D Poisson network. However, in low-reliability regime, it behaves like a 2-D Poisson network. The authors in [25] derive the outage probability of V2V communications at intersections in the presence of interference with a power control strategy.

In this line of research, we study the performance of V2V and V2I communications in intersection scenarios in presence of interference. However, all the aforementioned works that deal with intersection scenarios consider only a direct transmission, and assume independent interference, which is not always the case. They also consider that the receiving nodes are on the roads, which is not the case in V2I communications. As the best of the authors knowledge, there are no prior work that consider an intersection scenario with direct transmission when the received nodes can be anywhere on the plan, and a cooperative transmission considering vehicles mobility which result in dependent and independent interference.

*C-Contribution:*

In this paper, we focus on direct and cooperative transmissions for intersection scenarios in presence of interference. We develop a framework to model a direct transmission and a relayed transmission between vehicles (V2V) and between vehicles and infrastructure (V2I) at intersections using tools from stochastic geometry and point process theory. We derive the outage probability expression for a direct transmission, when the receiving node can be anywhere on the plan. We then derive the outage probability in a relayed transmission considering different decoding strategies, namely selection combining (SC) and maximal ratio combining (MRC). We also consider two mobility models. The first model is the low speed or static vehicles (LSV) model which assume that the interferer vehicles move slowly or not at all. The second model is the high speed vehicles (HSV) model which assume that the interferer vehicles move at high speed. The main contributions of our paper are:

- We develop a tractable analysis to model V2V and V2I communications for direct trans-

missions and for cooperative transmissions in intersection scenarios, and we show that cooperative transmissions always enhance the outage probability performance compared to direct transmissions. We study two mobility models, and compare their outage probability and throughput performance under different traffic densities.

- We evaluate the outage probability when the destination uses SC and MRC, and we show that MRC has a better performance over SC when the relay is close to the source. We also evaluate the outage probability for several relay positions, and we find the optimal relay position for different traffic conditions and vehicle mobility models; and we show that the outage probability does not improve after the number of infrastructure relays reached a threshold value.
- We derive a closed form of the outage probability when the interference are dependent and independent given specific channel conditions. We also obtained closed form of Laplace transform expressions where the relay and/or the destination are located anywhere on the plan, for specific channel conditions.
- We study the outage probability performance of cooperative transmissions in highways and intersection scenarios. We show that, as the vehicles move closer to intersections, the outage probability increases compared to highway scenarios. However, as the vehicles move away from intersections, highway and intersection scenarios exhibit the same performance, which confirms the statement that intersections are critical areas and more prone to incidents. Finally, we show that, depending on the environment, the interference dependence behaves differently. For instance, suburban intersections have a lower interference dependence compared to urban intersections. This is obtained by studying the impact of the path loss exponent on the outage probability performance.

#### *D-Organization:*

The rest of this paper is organized as follows. Section II presents our system model. In Section III, the outage behavior is carried out for several scenarios. The Laplace transform expressions are derived in Section IV. Simulation and discussion can be found in Section V. Finally, we conclude this paper in Section VI.

Notation: We denote  $\|\cdot\|$  the Euclidean norm.  $\mathbb{P}(A)$  denotes the probability of the event  $A$ .  $\mathcal{L}_I(\cdot)$  and  $\mathbb{E}_I[\cdot]$  denote the Laplace transform and the expectation with respect to the random variable  $I$ , respectively.  $\mathbb{1}\{\cdot\}$  denotes the indicator function.

## II. SYSTEM MODEL

Our aim is to compute the performance of a cooperative transmission in terms of outage probability between a source node  $S$  and a destination node  $D$ , with the help of a relay node  $R$ . For the sake of convenience, we use  $S$ ,  $D$  and  $R$  to denote both the nodes and their locations as depicted in Fig.1.

We consider an intersection case with two perpendicular roads, the horizontal road denoted by  $X$  and the vertical road denoted by  $Y$ . As we consider both V2V and V2I communications, any node of the triplet  $\{S, R, D\}$  can be on the road (as a vehicle) or outside the roads (as part of the communication infrastructure). As shown in Fig.1, the distance between the relay and the intersection (resp. between the destination and the intersection) is denoted by  $r$  (resp.  $d$ ), the intersection is the point when the road  $X$  and  $Y$  intersect, i.e., the point with the coordinate  $(0,0)$ .

We also consider a set of interfering vehicles that are located on the roads. We assume that the set of interfering vehicles on axis  $X$ , denoted by  $\Phi_X$  (resp. on axis  $Y$ , denoted by  $\Phi_Y$ ) are distributed according to a one-Dimensional Homogeneous Poisson Point Process (1D-HPPP) denoted by  $\Phi_X \sim 1D\text{-HPPP}(\lambda_X, x)$  (resp.  $\Phi_Y \sim 1D\text{-HPPP}(\lambda_Y, y)$ ) over the space  $\mathcal{B}$ , where  $x$  and  $\lambda_X$  (resp.  $y$  and  $\lambda_Y$ ) are the position of the interferer vehicles and their intensity on the  $X$  road (resp.  $Y$  road). We denote by  $x$  and  $y$ , both interferers and their locations. Finally, we consider that the 1D-HPPP can be on infinite road segments, i.e.,  $\mathcal{B} = \{x \in \mathbb{R}, y \in \mathbb{R}\}$ , or on a finite road segments, i.e.,  $\mathcal{B} = \{x, y \in \mathbb{R} \mid |x| < Z, |y| < Z\}$ .

The nodes use a slotted ALOHA protocol. The time axis is divided into time-slots and each transmitting node can access the medium at each time-slot with probability  $p \in [0, 1]$ , which performs an independent  $p$ -thinning of the original point process.

We use a Decode-and-Forward (DF) transmission scheme, i.e., the node  $R$  decodes and re-encodes the message then forwards it. We consider a half-duplex transmission, in which, a transmission occurs during two phases. The duration of each phase is one time-slot. In the first phase, the source broadcasts the message to the relay and destination ( $S \rightarrow R$  and  $S \rightarrow D$ ). In the second phase, we consider two decoding schemes. For the first one, named SC, the relay transmits to the destination ( $R \rightarrow D$ ). For the second one, named MRC, the relay transmits to the destination and the destination adds the power received from the relay and the power received from the source in the first time slot ( $R \rightarrow D$  and  $S \rightarrow D$ ). The transmission

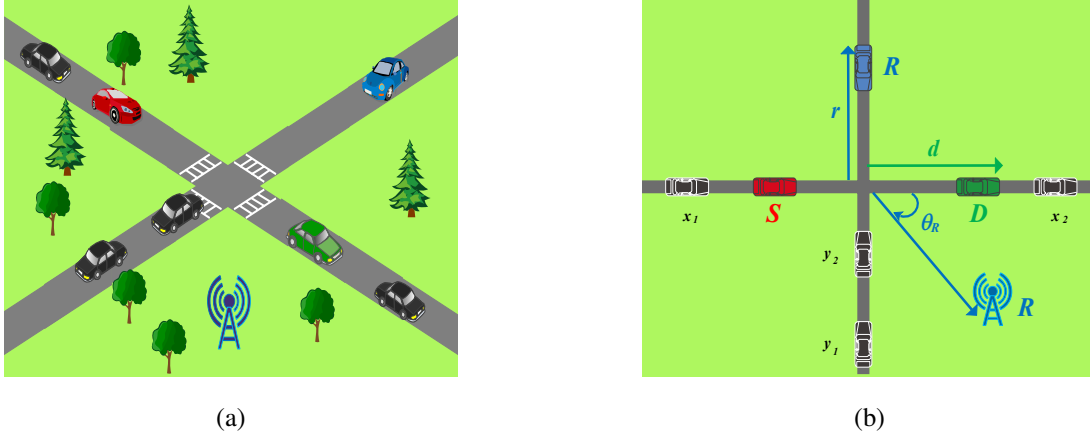


Fig. 1: system model

between any pair of two nodes  $a$  and  $b$  experiences a path loss  $l_{ab} = (Ar_{ab})^{-\alpha}$ , where  $A$  is a constant depending on the antenna characteristics,  $r_{ab}$  is the Euclidean distance between the node  $a$  and  $b$ , i.e.,  $r_{ab} = \|a - b\|$ , and  $\alpha$  is the path loss exponent. All nodes transmit with a constant power  $P$ .

The received signal at the relay and the destination can be expressed respectively as

$$\mathcal{Y}_R = h_{SR}\sqrt{l_{SR}P}\chi_S + \sum_{x \in \Phi_X} h_{Rx}\sqrt{l_{Rx}P}\chi_x + \sum_{y \in \Phi_Y} h_{Ry}\sqrt{l_{Ry}P}\chi_y + n_R$$

$$\mathcal{Y}_D = h_{SD}\sqrt{l_{SD}P}\chi_S + h_{RD}\sqrt{l_{RD}P}\chi_R + \sum_{x \in \Phi_X} h_{Dx}\sqrt{l_{Dx}P}\chi_x + \sum_{y \in \Phi_Y} h_{Dy}\sqrt{l_{Dy}P}\chi_y + n_D,$$

where  $\chi_S$  and  $\chi_R$  are the messages transmitted by  $S$  and  $R$ ,  $\mathcal{Y}_R$  and  $\mathcal{Y}_D$  are the messages received by  $R$  and  $D$  respectively. The messages transmitted by the interfere node  $x$  and  $y$  from the  $X$  and  $Y$  road, are denoted  $\chi_x$  and  $\chi_y$  respectively,  $h_{ab}$  is the fading coefficient between node  $a$  and  $b$ , and is modeled as  $\mathcal{CN}(0, 1)$  (Rayleigh fading). The power fading coefficient between the node  $a$  and  $b$ ,  $|h_{ab}|^2$ , follows an exponential distribution with unit mean,  $n_R$  and  $n_D$  are two additive with Gaussian noises (AWGN) with zero mean and variance  $\sigma^2$ . We define the aggregate

interference as

$$I_{X_R} = \sum_{x \in \Phi_{X_R}} P|h_{Rx}|^2 l_{Rx} \mathbb{1}\{x \in \Phi_{X_R}\} \quad (1)$$

$$I_{Y_R} = \sum_{y \in \Phi_{Y_R}} P|h_{Ry}|^2 l_{Ry} \mathbb{1}\{y \in \Phi_{Y_R}\} \quad (2)$$

$$I_{X_D} = \sum_{x \in \Phi_{X_D}} P|h_{Dx}|^2 l_{Dx} \mathbb{1}\{x \in \Phi_{X_D}\} \quad (3)$$

$$I_{Y_D} = \sum_{y \in \Phi_{Y_D}} P|h_{Dy}|^2 l_{Dy} \mathbb{1}\{y \in \Phi_{Y_D}\}, \quad (4)$$

where  $I_{X_R}$  is the aggregate interference from the X road at the relay,  $I_{Y_R}$  is the aggregate interference from the Y road at the relay,  $I_{X_D}$  is the aggregate interference from the X road at the destination,  $I_{Y_D}$  is the aggregate interference from the Y road at the destination,  $\Phi_{X_R}$  is the set of the interferers from the road X at the relay,  $\Phi_{Y_R}$  is the set of the interferers from the road Y at the relay,  $\Phi_{X_D}$  is the set of the interferers from the road X at the destination, and  $\Phi_{Y_D}$  is the set of the interferers from the road Y at the destination.

In this work, we consider two mobility models. In the first model, which we referred to as the low speed or static vehicles (LSV), we assume that the interferers (vehicles) do not move or move slowly, that is, their positions remain the same during the two time slots of the transmission. Thus the vehicles that interfere at the relay and at the destination are originated from the same set, i.e.,

$$\Phi_{X_R} = \Phi_{X_D} = \Phi_X,$$

and

$$\Phi_{Y_R} = \Phi_{Y_D} = \Phi_Y.$$

In the second model, which we referred to as the high speed vehicles (HSV), we assume that the vehicles move at a high speed, that is, their positions change every time slot. Thus, the vehicles that interfere at the relay are not the same that interfere at the destination, i.e.,

$$\Phi_{X_R} \cap \Phi_{X_D} = \emptyset,$$

and

$$\Phi_{Y_R} \cap \Phi_{Y_D} = \emptyset.$$

### III. OUTAGE COMPUTATION

#### A. Condition for outage:

We define, in this section, the outage events related to the DF protocol using a half-duplex transmission. We first define the outage event related to the direct link  $S - D$ . Then, we define the outage events related to the relayed links  $S - R$  and  $R - D$  when using SC and MRC.

1) *Direct transmission:* We define the rate related to the direct link  $S - D$ , denoted  $\mathcal{R}_{SD}$ , as

$$\mathcal{R}_{SD} = \frac{1}{2} \log_2 \left[ 1 + \frac{P|h_{SD}|^2 l_{SD}}{\sigma^2 + I_{X_D} + I_{Y_D}} \right]. \quad (5)$$

We define the outage event on the direct link  $S - D$ , denoted  $O_{SD}$ , as

$$O_{SD} \triangleq [\mathcal{R}_{SD} < \mathcal{R}], \quad (6)$$

where  $\mathcal{R}$  is the target rate.

2) *Relayed transmission:* We define the rates related to the relayed link  $S - R$  and  $R - D$ , denoted respectively  $\mathcal{R}_{SR}$  and  $\mathcal{R}_{RD}$ , as

$$\mathcal{R}_{SR} = \frac{1}{2} \log_2 \left[ 1 + \frac{P|h_{SR}|^2 l_{SR}}{\sigma^2 + I_{X_R} + I_{Y_R}} \right], \quad (7)$$

and

$$\mathcal{R}_{RD} = \frac{1}{2} \log_2 \left[ 1 + \frac{P|h_{RD}|^2 l_{RD}}{\sigma^2 + I_{X_D} + I_{Y_D}} \right]. \quad (8)$$

We now define the outage events on the relayed link  $S - R$  and  $R - D$  as

$$O_{SR} \triangleq [\mathcal{R}_{SR} < \mathcal{R}] \quad (9)$$

$$O_{RD} \triangleq [\mathcal{R}_{RD} < \mathcal{R}]. \quad (10)$$

Notice that the outage can also be expressed in terms of signal-to-interference-plus-noise ratio (SINR), that is, an outage event occurs when the SINR is lower than a decoding threshold  $\theta$ , which can be expressed by

$$\text{SINR}_{ab} < \theta,$$

where  $\text{SINR}_{ab} = \frac{P|h_{ab}|^2 l_{ab}}{\sigma^2 + I_{X_b} + I_{Y_b}}$ ,  $\theta = 2^{2\mathcal{R}} - 1$ , and  $a$  and  $b$  are the transmitting and the receiving node, respectively.

Since we use SC and MRC, we have two expressions of the outage event during the second phase. In SC, an outage event occurs when the destination cannot decode the source message, and



cannot decode the relay message given that the relay successfully decoded the source message. In MRC, an outage event occurs when the destination cannot decode the source message, and cannot decode the message when adding the relay and the source power given that the relay successfully decoded the source message.

Therefore, we express the outage  $O_{SC}$  for SC as

$$O_{SC} = [O_{SR} \cap O_{SD}] \cup [O_{SR}^C \cap O_{RD}], \quad (11)$$

where  $O_{SR}^C \triangleq [\mathcal{R}_{SR} > \mathcal{R}]$  is the event that the relay successfully decodes the source message.

We express the outage  $O_{MRC}$  for MRC as

$$O_{MRC} = [O_{SR} \cap O_{SD}] \cup [O_{SR}^C \cap O_{SRD}], \quad (12)$$

where  $O_{SRD} \triangleq [\mathcal{R}_{SRD} < \mathcal{R}]$  is the outage event at the destination when the relay and the source transmit simultaneously, and  $\mathcal{R}_{SRD}$  the rate when using MRC. The rate  $\mathcal{R}_{SRD}$  is expressed as

$$\mathcal{R}_{SRD} = \frac{1}{2} \log_2 \left[ 1 + \frac{P|h_{SD}|^2 l_{SD} + P|h_{RD}|^2 l_{RD}}{\sigma^2 + I_{X_D} + I_{Y_D}} \right]. \quad (13)$$

### B. Outage behaviour:

In this section, we calculate the outage probability for the direct transmission and the relayed transmission.

1) *Direct transmission:* The outage probability for the direct transmission using DF protocol and half-duplex transmission is expressed as

$$\begin{aligned} \mathbb{P}(O_{SD}) &= 1 - N_{SD} \mathbb{E}_{I_X} [\exp(-K_{SD} I_{X_D})] \mathbb{E}_{I_Y} [\exp(-K_{SD} I_{Y_D})] \\ &= 1 - N_{SD} \mathcal{L}_{I_{X_D}}(K_{SD}) \mathcal{L}_{I_{Y_D}}(K_{SD}), \end{aligned} \quad (14)$$

where  $K_{ab} = \frac{\theta}{Pl_{ab}}$  and  $N_{ab} = \exp(-K_{ab}\sigma^2)$ .

2) *Relayed transmission:* The outage probability for the DF protocol using a half-duplex transmission when the destination uses SC,  $\mathbb{P}(O_{SC})$  is

$$\mathbb{P}(O_{SC}) = \mathbb{P}(O_{SR} \cap O_{SD}) + \mathbb{P}(O_{SR}^C \cap O_{RD}), \quad (15)$$

and the outage probability when the destination uses MRC,  $\mathbb{P}(O_{MRC})$  is

$$\mathbb{P}(O_{MRC}) = \mathbb{P}(O_{SR} \cap O_{SD}) + \mathbb{P}(O_{SR}^C \cap O_{SRD}). \quad (16)$$

For the sake of convenience, we will express the outage probability  $\mathbb{P}(\mathcal{O}_{SC})$  as a function of the success probability  $\mathbb{P}(\mathcal{O}_{SC}^C)$  for SC as

$$\mathbb{P}(\mathcal{O}_{SC}) = 1 - \mathbb{P}(\mathcal{O}_{SC}^C), \quad (17)$$

and  $\mathbb{P}(\mathcal{O}_{MRC})$  for MRC as

$$\mathbb{P}(\mathcal{O}_{MRC}) = 1 - \mathbb{P}(\mathcal{O}_{MRC}^C). \quad (18)$$

As for the outage probability, the success probability has two expressions, depending whether the destination uses SC or MRC. When the destination uses SC, the success probability  $\mathbb{P}(\mathcal{O}_{SC}^C)$  is

$$\mathbb{P}(\mathcal{O}_{SC}^C) = \mathbb{P}(\mathcal{O}_{SR} \cap \mathcal{O}_{SD}^C) + \mathbb{P}(\mathcal{O}_{SR}^C \cap \mathcal{O}_{RD}^C), \quad (19)$$

and when the destination uses MRC the success probability  $\mathbb{P}(\mathcal{O}_{MRC}^C)$  is

$$\mathbb{P}(\mathcal{O}_{MRC}^C) = \mathbb{P}(\mathcal{O}_{SR} \cap \mathcal{O}_{SD}^C) + \mathbb{P}(\mathcal{O}_{SR}^C \cap \mathcal{O}_{SRD}^C). \quad (20)$$

Now, we calculate each probability in equations (19) and (20). First, we calculate the probability  $\mathbb{P}(\mathcal{O}_{SR} \cap \mathcal{O}_{SD}^C)$ , this probability is related to the outage during the first phase, its expression does not change whether the destination uses SC or MRC. The expression of  $\mathbb{P}(\mathcal{O}_{SR} \cap \mathcal{O}_{SD}^C)$  is given by

$$\begin{aligned} \mathbb{P}(\mathcal{O}_{SR} \cap \mathcal{O}_{SD}^C) &= N_{SD} \mathbb{E}_{I_X} [\exp(-K_{SD} I_{X_D})] \mathbb{E}_{I_Y} [\exp(-K_{SD} I_{Y_D})] - \\ &N_{SR} N_{SD} \mathbb{E}_{I_X} [\exp(-K_{SR} I_{X_R} - K_{SD} I_{X_D})] \mathbb{E}_{I_Y} [\exp(-K_{SR} I_{Y_R} - K_{SD} I_{Y_D})], \end{aligned} \quad (21)$$

*Proof:* See Appendix A. ■

The outage probability during the second phase has two expressions, depending on the transmission scheme. The outage probability, when using SC, denoted  $\mathbb{P}(\mathcal{O}_{SR}^C \cap \mathcal{O}_{RD}^C)$ , is expressed as

$$\mathbb{P}(\mathcal{O}_{SR}^C \cap \mathcal{O}_{RD}^C) = N_{SR} N_{RD} \mathbb{E}_{I_X} [\exp(-K_{SR} I_{X_R} - K_{RD} I_{X_D})] \mathbb{E}_{I_Y} [\exp(-K_{SR} I_{Y_R} - K_{RD} I_{Y_D})]. \quad (22)$$

*Proof:* See Appendix B. ■

The outage probability, when using MRC, denoted  $\mathbb{P}(\mathcal{O}_{SR}^C \cap \mathcal{O}_{SRD}^C)$  is given by

$$\begin{aligned} \mathbb{P}(\mathcal{O}_{SR}^C \cap \mathcal{O}_{SRD}^C) &= \\ &\frac{N_{SR} N_{RD} l_{RD}}{l_{RD} - l_{SD}} \mathbb{E}_{I_X} [\exp(-K_{SR} I_{X_R} - K_{RD} I_{X_D})] \mathbb{E}_{I_Y} [\exp(-K_{SR} I_{Y_R} - K_{RD} I_{Y_D})] \end{aligned}$$

$$- \frac{N_{SR}N_{SD}l_{SD}}{l_{RD} - l_{SD}} \mathbb{E}_{I_X}[\exp(-K_{SR}I_{X_R} - K_{SD}I_{X_D})] \mathbb{E}_{I_Y}[\exp(-K_{SR}I_{Y_R} - K_{SD}I_{Y_D})]. \quad (23)$$

*Proof:* See Appendix C. ■

We can notice that equation (23) is not defined when  $l_{RD} = l_{SD}$ . However, we do not calculate the outage probability in this case.

Note that the outage probability expressions derived before are expressed as a function of the expectation with respect to  $I_X$  and  $I_Y$ . The expression of the expectation changes depending on the vehicles mobility models, i.e., the HSV and the LSV models.

**Theorem 1.** *The outage probability for the HSV model using SC and MRC is given by (17) and (18), where  $\mathbb{P}(\mathcal{O}_{SR} \cap \mathcal{O}_{SD}^C)$  in (19) is given by*

$$\mathbb{P}(\mathcal{O}_{SR} \cap \mathcal{O}_{SD}^C) = N_{SD} \mathcal{L}_{I_{X_D}}(K_{SD}) \mathcal{L}_{I_{Y_D}}(K_{SD}) - N_{SR} N_{SD} \mathcal{L}_{I_{X_R}}(K_{SR}) \mathcal{L}_{I_{Y_R}}(K_{SR}) \mathcal{L}_{I_{X_D}}(K_{SD}) \mathcal{L}_{I_{Y_D}}(K_{SD}). \quad (24)$$

The probability  $\mathbb{P}(\mathcal{O}_{SR}^C \cap \mathcal{O}_{RD}^C)$  and  $\mathbb{P}(\mathcal{O}_{SR}^C \cap \mathcal{O}_{SRD}^C)$  in (19) and (20) are respectively expressed by

$$\mathbb{P}(\mathcal{O}_{SR}^C \cap \mathcal{O}_{RD}^C) = N_{SR} N_{RD} \mathcal{L}_{I_{X_R}}(K_{SR}) \mathcal{L}_{I_{Y_R}}(K_{SR}) \mathcal{L}_{I_{X_D}}(K_{RD}) \mathcal{L}_{I_{Y_D}}(K_{RD}), \quad (25)$$

and

$$\mathbb{P}(\mathcal{O}_{SR}^C \cap \mathcal{O}_{SRD}^C) = \frac{N_{SR} N_{RD} l_{RD}}{l_{RD} - l_{SD}} \mathcal{L}_{I_{X_R}}(K_{SR}) \mathcal{L}_{I_{Y_R}}(K_{SR}) \mathcal{L}_{I_{X_D}}(K_{RD}) \mathcal{L}_{I_{Y_D}}(K_{RD}) - \frac{N_{SR} N_{SD} l_{SD}}{l_{RD} - l_{SD}} \mathcal{L}_{I_{X_R}}(K_{SR}) \mathcal{L}_{I_{Y_R}}(K_{SR}) \mathcal{L}_{I_{X_D}}(K_{SD}) \mathcal{L}_{I_{Y_D}}(K_{SD}). \quad (26)$$

*Proof:* See Appendix D. ■

**Theorem 2.** *The outage probability for the LSV model using SC and MRC is given by (17) and (18), where  $\mathbb{P}(\mathcal{O}_{SR} \cap \mathcal{O}_{SD}^C)$  in (19) is given by*

$$\mathbb{P}(\mathcal{O}_{SR} \cap \mathcal{O}_{SD}^C) = N_{SD} \mathcal{L}_{I_{X_D}}(K_{SD}) \mathcal{L}_{I_{Y_D}}(K_{SD}) - N_{SD} N_{SR} \mathcal{L}_{I_{X_R}, I_{X_D}}(K_{SR}, K_{SD}) \mathcal{L}_{I_{Y_R}, I_{Y_D}}(K_{SR}, K_{SD}). \quad (27)$$

The probability  $\mathbb{P}(\mathcal{O}_{SR}^C \cap \mathcal{O}_{RD}^C)$  and  $\mathbb{P}(\mathcal{O}_{SR}^C \cap \mathcal{O}_{SRD}^C)$  in (19) and (20) are respectively given by

$$\mathbb{P}(\mathcal{O}_{SR}^C \cap \mathcal{O}_{RD}^C) = N_{SR} N_{RD} \mathcal{L}_{I_{X_R}, I_{X_D}}(K_{SR}, K_{RD}) \mathcal{L}_{I_{Y_R}, I_{Y_D}}(K_{SR}, K_{RD}), \quad (28)$$

and

$$\mathbb{P}(\mathcal{O}_{SR}^C \cap \mathcal{O}_{SRD}^C) = \frac{N_{SR}N_{RD}l_{RD}}{l_{RD} - l_{SD}} \mathcal{L}_{I_{X_R}, I_{X_D}}(K_{SR}, K_{RD}) \mathcal{L}_{I_{Y_R}, I_{Y_D}}(K_{SR}, K_{RD}) - \frac{N_{SR}N_{SD}l_{SD}}{l_{RD} - l_{SD}} \mathcal{L}_{I_{X_R}, I_{X_D}}(K_{SR}, K_{SD}) \mathcal{L}_{I_{Y_R}, I_{Y_D}}(K_{SR}, K_{SD}), \quad (29)$$

where

$$\mathcal{L}_{I_{X_R}, I_{X_D}}(s, b) = \mathcal{L}_{I_{X_R}}(s) \mathcal{L}_{I_{X_D}}(b) \rho_X(s, b) \quad (30)$$

$$\mathcal{L}_{I_{Y_R}, I_{Y_D}}(s, b) = \mathcal{L}_{I_{Y_R}}(s) \mathcal{L}_{I_{Y_D}}(b) \rho_Y(s, b) \quad (31)$$

$$\rho_X(s, b) = \exp \left( p \lambda_X \int_{\mathcal{B}} \frac{sbP^2 l_{Rx} l_{Dx}}{(1 + sPl_{Rx})(1 + bPl_{Dx})} dx \right) \quad (32)$$

$$\rho_Y(s, b) = \exp \left( p \lambda_Y \int_{\mathcal{B}} \frac{sbP^2 l_{Ry} l_{Dy}}{(1 + sPl_{Ry})(1 + bPl_{Dy})} dy \right). \quad (33)$$

*Proof:* See Appendix E. ■

The cross term  $\rho_X(s, b)$  and  $\rho_Y(s, b)$  arise from the dependence between the interference at two locations (the relay and the destination). Fortunately, in our scenario, a closed form for the cross terms  $\rho_X(s, b)$  and  $\rho_Y(s, b)$  can be obtained for  $\alpha = 2$  and  $\alpha = 4$ , in the case when the interference are originated from vehicles in finite and infinite road segments.

#### IV. LAPLACE TRANSFORM EXPRESSIONS

After we obtained the expressions of the outage probability, we derive, in this section, the Laplace transform expressions of the interference from the X road and from the Y road when the interference are originated from vehicles in finite road segments ( $\mathcal{B} = [-Z, Z]$ ), and infinite road segments ( $\mathcal{B} = \mathbb{R}$ ). As mentioned in the previous section, joint Laplace transforms can be expressed as the product of two Laplace transforms and a cross term. A closed form expression of the cross term can be obtained for  $\alpha = 2$  and  $\alpha = 4$ . However, they will not be presented here due to space limitation. Thus, in this section, we are only concerned with the computation of the single Laplace transform.

The Laplace transform of the interference originating from the X road at the received node denoted  $N$ , is expressed as

$$\mathcal{L}_{I_{X_N}}(s) = \exp \left( -p \lambda_X \int_{\mathcal{B}} \frac{1}{1 + (A\|x - N\|^\alpha)/sP} dx \right), \quad (34)$$

and

$$\|x - N\| = \sqrt{(n \sin(\theta_N))^2 + (x - n \cos(\theta_N))^2}. \quad (35)$$

The Laplace transform of the interference originating from the Y road is given by

$$\mathcal{L}_{I_{Y_N}}(s) = \exp \left( -p\lambda_Y \int_{\mathcal{B}} \frac{1}{1 + (A\|y - N\|^\alpha)/sP} dy \right), \quad (36)$$

where

$$\|y - N\| = \sqrt{(n \cos(\theta_N))^2 + (y - n \sin(\theta_N))^2}, \quad (37)$$

where  $n$  and  $\theta_N$  are the distance between the node  $N$  and the intersection, and the angle between the node  $N$  and the X road, respectively.

The expression (34) and (36) do not have a closed form. Fortunately, we can obtain a closed form for  $\alpha = 2$  and  $\alpha = 4$  when  $\mathcal{B} = \mathbb{R}$ , and  $\mathcal{B} = [-Z, Z]$ . However, the case when  $\alpha = 4$  will not be presented here due to the lack of space.

**Proposition 1.** *The Laplace transform expressions of the interference at the node  $N$  for an intersection scenario, when  $\mathcal{B} = \mathbb{R}$ , and when  $\alpha = 2$  are given by*

$$\mathcal{L}_{I_{X_N}}(s) = \exp \left( -p\lambda_X \frac{sP}{A^2} \frac{\pi}{\sqrt{(n \sin(\theta_N))^2 + sP/A^2}} \right), \quad (38)$$

and

$$\mathcal{L}_{I_{Y_N}}(s) = \exp \left( -p\lambda_Y \frac{sP}{A^2} \frac{\pi}{\sqrt{(n \cos(\theta_N))^2 + sP/A^2}} \right). \quad (39)$$

*Proof:* See Appendix F. ■

When a cooperative transmission is considered,  $N \in \{R, D\}$  and  $n \in \{r, d\}$ .

Note that when  $\theta_N = 0$ , it corresponds to the case where the received node is on the X road. Then, if we substitute  $\theta_N = 0$  in (38) and (39), we obtain the special case in [21] when the receiving node is on the X road, and when the direct transmission and infinite road segments are considered

$$\begin{aligned} \mathcal{L}_{I_X}(s) &= \exp \left( -p\lambda_X \pi \sqrt{sP}/A \right) \\ \mathcal{L}_{I_Y}(s) &= \exp \left( -p\lambda_Y \frac{\sqrt{sP}}{A} \frac{\pi}{\sqrt{1 + (An/\sqrt{sP})^2}} \right). \end{aligned}$$

**Proposition 2.** *The Laplace transform expressions of the interference at the node  $N$  for an intersection scenario, when  $\mathcal{B} = [-Z, Z]$  and when  $\alpha = 2$  are given by*

$$\mathcal{L}_{I_{X_N}}(s) = \exp(-p\lambda_X\Theta_X(s)), \quad (40)$$

and

$$\mathcal{L}_{I_{Y_N}}(s) = \exp(-p\lambda_Y\Theta_Y(s)), \quad (41)$$

where

$$\Theta_X(s) = \frac{\arctan\left(\frac{Z+n_x}{\sqrt{n_y^2+sP/A^2}}\right) + \arctan\left(\frac{Z-n_x}{\sqrt{n_y^2+sP/A^2}}\right)}{\frac{A^2}{sP}\sqrt{n_y^2+\frac{sP}{A^2}}}, \quad (42)$$

and

$$\Theta_Y(s) = \frac{\arctan\left(\frac{Z+n_y}{\sqrt{n_x^2+sPA^2}}\right) + \arctan\left(\frac{Z-n_y}{\sqrt{n_x^2+sPA^2}}\right)}{\frac{A^2}{sP}\sqrt{n_x^2+\frac{sP}{A^2}}}. \quad (43)$$

*Proof:* See Appendix E. ■

It is worth noting that the expression of (38) does not depend on  $n\cos(\theta_N)$ , that is  $n_x$ . Similarly, (39) does not depend on  $n\sin(\theta_N)$ , that is  $n_y$ . However, one can notice that, (42) and (43) both depend on  $n_x$  and on  $n_y$ . This can be explained by the fact that, as interferers extend to infinity, the term  $(x-n_x)$  will tend to  $x$ , that is  $(x-n_x) \rightarrow x$  when  $x \rightarrow \infty$ , and  $(y-n_y) \rightarrow y$  when  $y \rightarrow \infty$ . This is no longer the case when the interferers are on finite road segments. In this case, the result depends on  $n_x$  and on  $n_y$ .

Now that the Laplace transform equations are at hand, we plug them into the outage probability equations, and we get the final and complete expressions of the outage probabilities.

## V. SIMULATIONS AND DISCUSSIONS

In this section, we evaluate the performance of our model and in order to verify the accuracy of the theoretical results, Monte Carlo simulations are obtained by averaging over 10,000 realizations of the PPPs and fading parameters. Unless stated otherwise, all the figures are plot for intersection scenarios. We set our simulation area to  $[-10^6 \text{ m}, 10^6 \text{ m}]$  for each road segment. We also set  $A = 650$ , and the transmit power to  $P = 120 \text{ mW}$ . Without loss of generality, we set

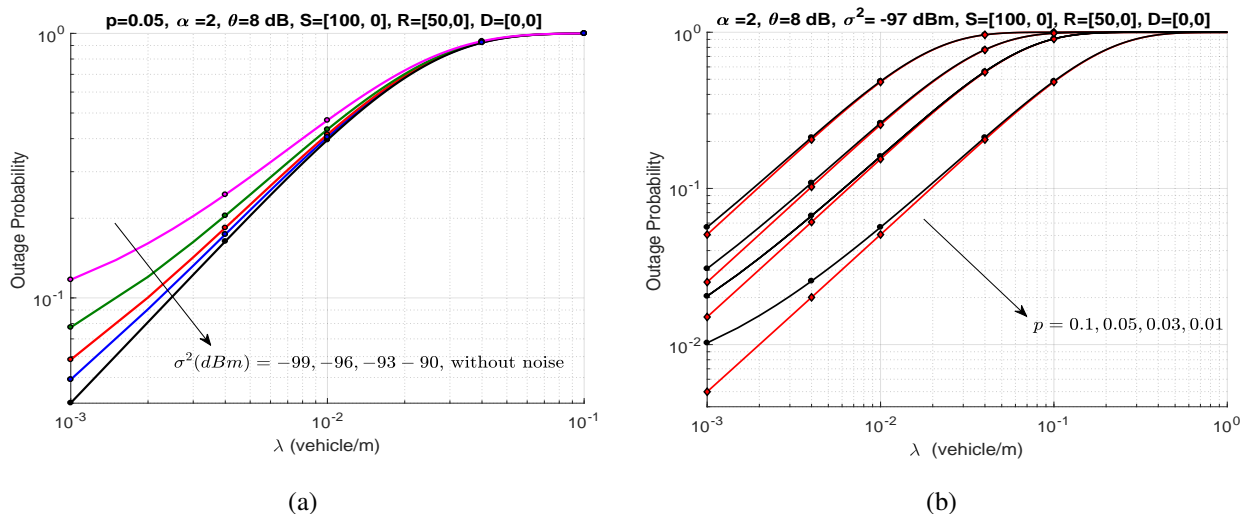


Fig. 2: Outage probability when the vehicles intensity  $\lambda$  considering SC and the HSV model. (a) represents the outage probability for several values of noise power level. (b) represents the outage probability for several values of  $p$  with noise (circle), and without noise (diamond).

$\lambda_X = \lambda_Y = \lambda$ . The vehicles intensity  $\lambda$  can also be interpreted as the average distance between vehicles.

Fig. 2-a plots the outage probability for several values of noise power level when  $p = 0.05$ . We can see from the figure that for low interference level (low vehicle intensity), the noise becomes predominant, and thus degrading the performance. However, as the level of interference becomes high, the noise becomes negligible. Fig. 2-b depicts the outage probability for several values of  $p$  when the noise power level is set to  $\sigma^2 = -97$  dBm. We can notice that, as  $p$  increases, the performance of the outage with noise and without noise converge to the same values. This is because, as  $p$  increases, the power of interference increases accordingly, thus making the power of noise negligible compared the interference power, which corresponds to the interference limited scenario.

In the next figures, since we are mainly interested in the effect of the interference, we will consider only the interference limited scenario, that is,  $\sigma^2 = 0$ .

From Fig.3, we can make the following observations. First, cooperative transmissions outperform the direct transmission, that is, the outage probability for a cooperative transmission is lower than the one for a direct transmission. Second, MRC outperforms SC. The explanation of the first observation is that, when the direct transmission fails, i.e., the link  $S$ - $D$  is in outage,

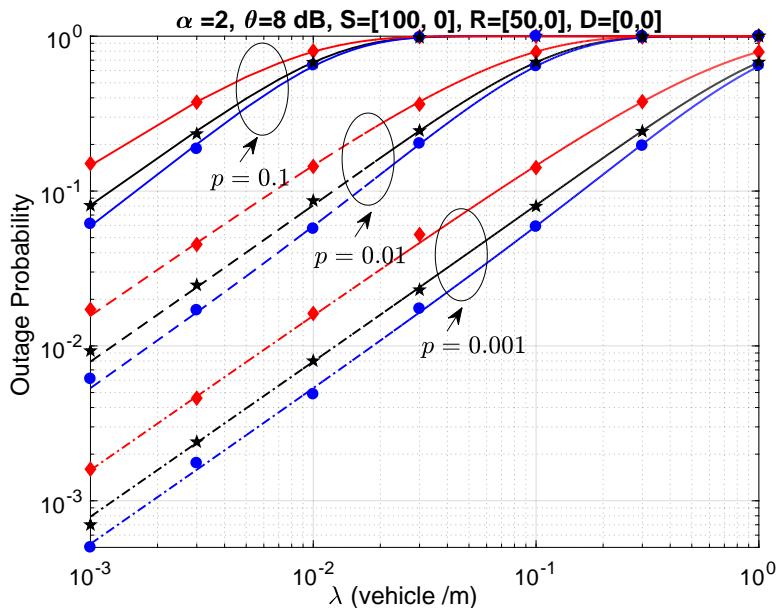


Fig. 3: Outage probability when varying  $\lambda$  for different values of  $p$  using the direct transmission scenario (diamond), and cooperative transmissions considering SC (star) and MRC (circle), for the HSV model.

it is unlikely that  $S-R$  and  $R-D$  are in outage too. Thus, the direct transmission is aided by the relaying paths  $S-R$  and  $R-D$ , and therefore the cooperative transmission always enhance the performance compared to the direct transmission. The explanation of the second observation is the well known fact that, in SC, the destination uses power received from the relay to decode the message. However, in MRC, the destination adds the relay power and the source power, which increases the SINR, and decreases the outage probability compared to SC. We notice that, for lower values of  $p$ , the outage probability decreases. This is because lower values of  $p$  mean lower probability for the vehicles to access the medium, leading to less interferers, and thus reducing the SINR and the outage probability. We can conclude that vehicles should always cooperate in order to minimize the outage probability, and we confirm the well known fact that, using MRC always enhance the performance compared to SC. We study the effect of MRC in Fig.6.

We notice from Fig.4 that, when the intensity of vehicles  $\lambda$  or  $p$  increase, the outage probability increases accordingly (as explained in Fig.3). We also notice that, for lower values of  $\lambda$  (low traffic conditions), the HSV model outperforms the LSV model. But, as the intensity of vehicles increases (high traffic conditions), the LSV model exhibits better performance. This is explained by the fact that the interference dependence (LSV) in high traffic is beneficial due to highly dependent hops of the relaying path. So, if the  $S-R$  link succeeded, it is likely to be the case of



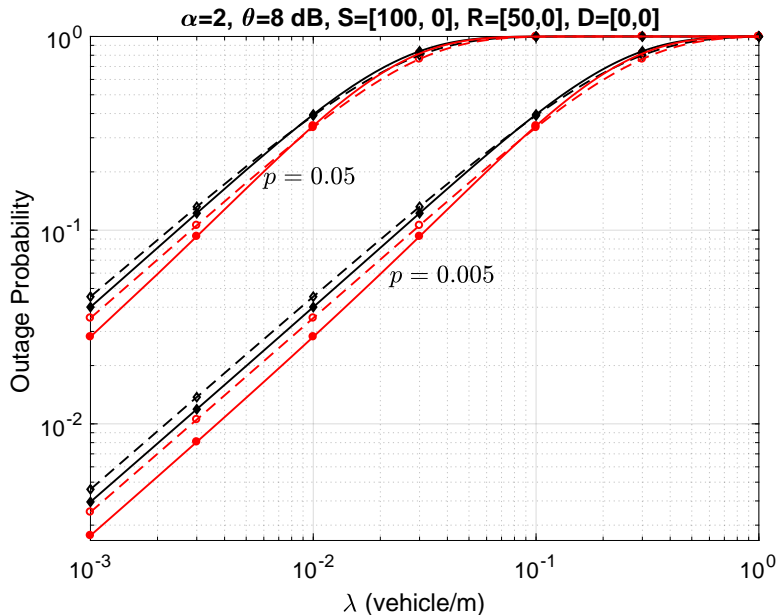


Fig. 4: Outage probability as a function of  $\lambda$  considering SC (diamond), and MRC (circle), for the HSV model (simple line) and the LSV model(dashed line).

the  $R$ - $D$  link. Thus, the interference dependence (LSV) leads to higher performance than in the presence of independent interference (HSV) in high traffic conditions, that is, when the number of transmitting vehicles increases [3]. In other words, in low traffic conditions, increasing the vehicle speed increases the outage performance, whereas in high traffic conditions, decreasing the vehicle speed increases the performance.

In Fig. 5, we plot the throughput as a function of  $\theta$ , where the throughput  $\mathcal{T}$  is defined as follows

$$\mathcal{T} = \mathbb{P}(O^C) \log_2(1 + \theta),$$

where  $\log_2(1 + \theta)$  is the Shannon bound (in nats per hertz) and  $\mathbb{P}(O^C)$  is the success probability [6]. We can notice that in a high traffic scenario ( $\lambda = 0.1$ ,  $\lambda = 0.2$ ), the LSV model allows the highest throughput than the HSV model. This confirms what we concluded in Fig. 4. We also notice that, in a low traffic scenario ( $\lambda = 0.01$ ,  $\lambda = 0.02$ ), the HSV model allows a slightly higher throughput than the LSV model. However, even for lower values of  $\lambda$  (low traffic), as  $\theta$  increases, the LSV model achieves a higher throughput than the HSV model. This is because, for larger values of  $\theta$ , in order to have an outage, a large number of vehicles have to transmit at the same time, hence, increasing traffic density.

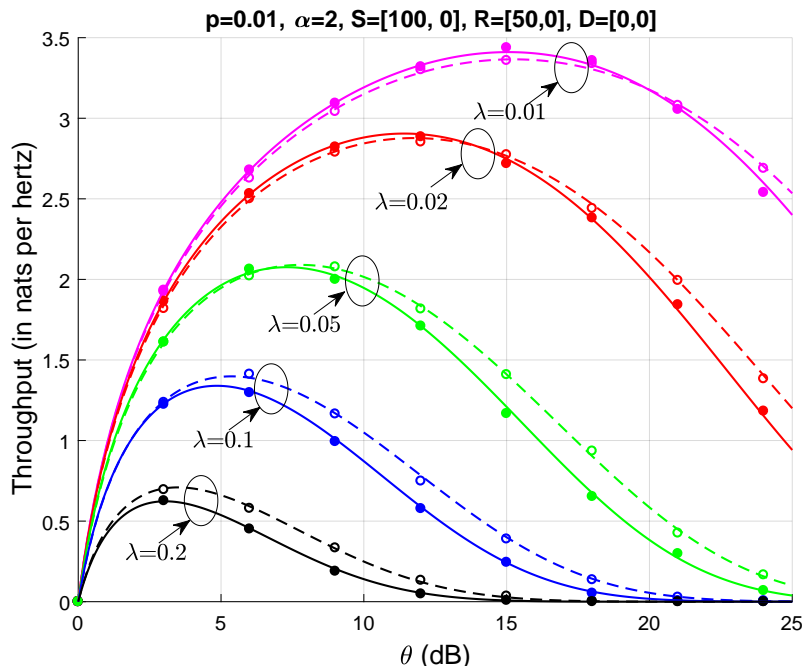


Fig. 5: Throughput as a function of  $\theta$  for different values of  $\lambda$  considering MRC, for the HSV model (simple line) and the LSV model (dashed line). Simulation results are represented with dots.

Note that  $\mathcal{T}$  is a function of  $\log_2(1 + \theta)$  and  $\mathbb{P}(O^C)$ . When  $\theta$  increases,  $\log_2(1 + \theta)$  increases. However, the success probability  $\mathbb{P}(O^C)$  decreases. In one hand, we are tempted to increase  $\theta$  to increase the rate. But on the other hand, increasing  $\theta$  increases the outage probability. An optimal value of  $\theta$  must be carefully set in order to maximize the throughput under given traffic conditions and vehicles mobility.

In Fig. 6, we plot the outage probability as a function of the relay position for a setting where  $S = (0, 0)$  and  $D = (200, 0)$ . We can see from Fig. 6-a that the best relay position for the LSV model is in the middle of  $S$  and  $D$ , whereas, the best relay position for the HSV model is slightly shifted from the middle toward  $D$ . We also can see from Fig. 6-a that, in high traffic scenarios, the LSV model achieves a better performance (as stated in Fig.4). However, when the relay is close to the destination, the HSV model has a better performance than the LSV model. This is because, in a high traffic scenario (harsh environment), the direct link  $S$ - $D$  is more likely to be in outage, therefore when the relay is close to the destination, that is,  $\|S - R\| \approx \|S - D\|$ , the  $S$ - $R$  link is more likely to be in outage due to highly dependent interference. Furthermore, as stated in Fig.4, in low traffic scenario, the HSV model has a better performance than the

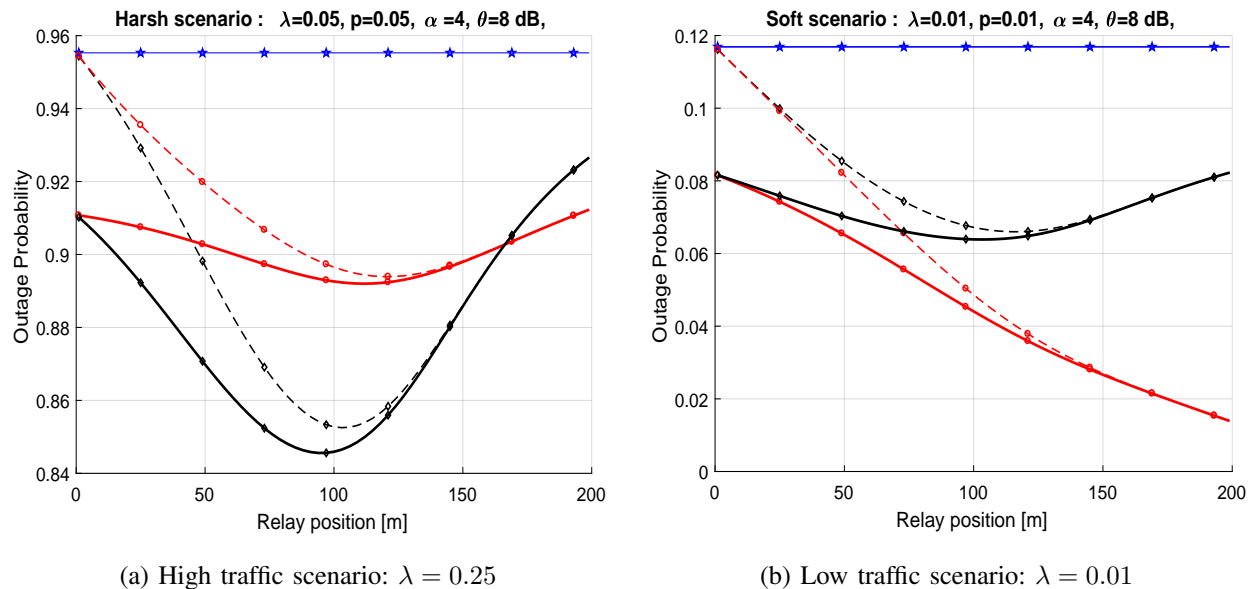


Fig. 6: Outage probability as a function of the relay position, considering SC (dashed line), MRC (line) and the direct transmission (star), for the HSV model(circle) and the LSV model(diamond).

LSV model. We can notice from Fig. 6-b that the best relay position for the HSV model is close to the destination whereas the best relay position for the LSV model is when the relay is equidistant from  $S$  and  $D$ . The explanation is as follow: in low traffic scenarios, the direct link has a high success probability in the presence of low interference level. However, in the HSV model, even if the direct link fails, it is less likely that the relay path fails too, since there is no dependence between interference. Hence, when the relay moves toward the destination, it increases the diversity gain and enhances the performance. This makes the best relay position in the HSV model close to the destination. However, in the LSV model, when the direct link fails, it is more likely that the relay path fails due to (low but still present) interference dependence. Hence, the best relay position is when the relay is equidistant from  $S$  and  $D$ .

Finally, we can notice, regardless of traffic conditions or vehicle speeds that, as the relay moves closer to the destination, MRC and SC offer the same performance. This is because, when the relay is close to the destination, the power received at the destination from the source is much smaller than the power received from the relays ( $l_{RD} \gg l_{SD}$ ). Thus, adding the power of  $S$ - $D$  link does not add much power (diversity gain) to the  $R$ - $D$  link, which makes MRC and SC at the same level of performance. When the relay is closer to the source, the level of power received at the destination from source and from the relay is almost the same ( $l_{RD} \approx l_{SD}$ ), which increases

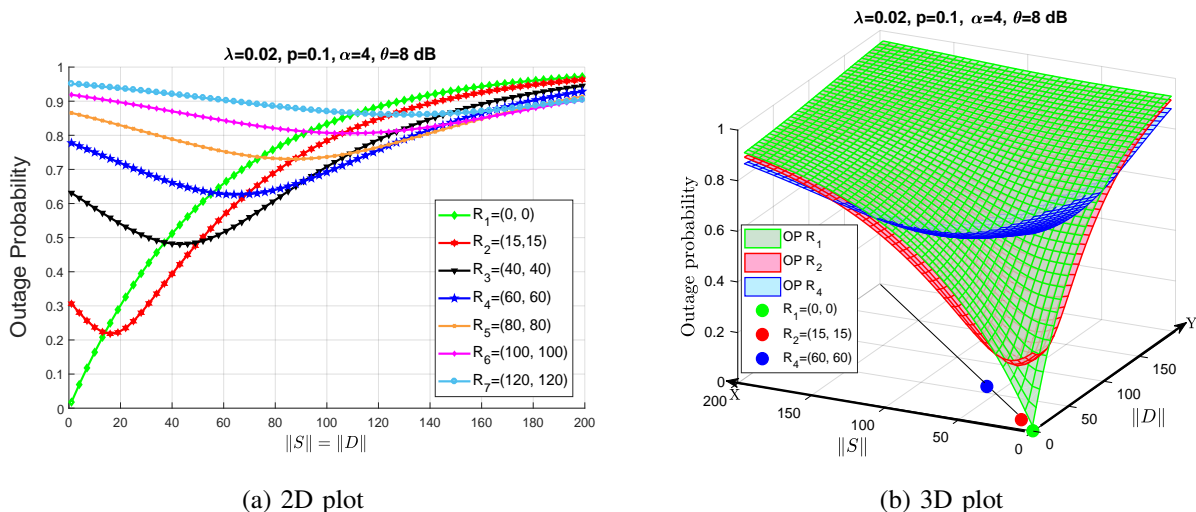


Fig. 7: Outage probability when varying the distance of the destination and the source from the intersection, denoted respectively  $\|S\|$  and  $\|D\|$  for several locations of the relay at the first bisector, in the LSV model. (a) represents the 2 dimensions plot, and (b) represents the 3 dimensions plot.

the diversity gain, leading to greater performance of MRC over SC.

The relay location plays an important role in the performance. This can be used in the relay-selection based algorithms, where vehicles have to take into account both the relays location and speeds (HSV or LSV). As regards the decoding strategies, there is also a tradeoff between performance and complexity to consider, because MRC is difficult to implement, and it is only beneficial when the relay is close to the source.

In Fig. 7, we present analytical results when the relay is located on the first bisector. We plot the outage probability as a function of the distance of the source from the intersection, and the distance of the destination from the intersection, denoted respectively  $\|S\|$  and  $\|D\|$ , in 2D (a) and 3D (b). Without loss of generality, we set the source on the X road, and the destination on the Y road.

Since the relay is outside the roads, we can consider that it belongs to the roadside infrastructure. A roadside infrastructure with the coordinate  $(0,0)$  can be placed in the center of a roundabout, or mounted on a traffic light pole. We can notice that the outage probability reaches its minimum when the relay is the middle of  $S$  and  $D$  (Fig.6). We also notice that there is no need to use a relay that would be farther than the coordinate  $(60,60)$  in terms of outage performance. Although there is a little bit of (but still negligible) gain when using  $R_3$ , we can state that using only

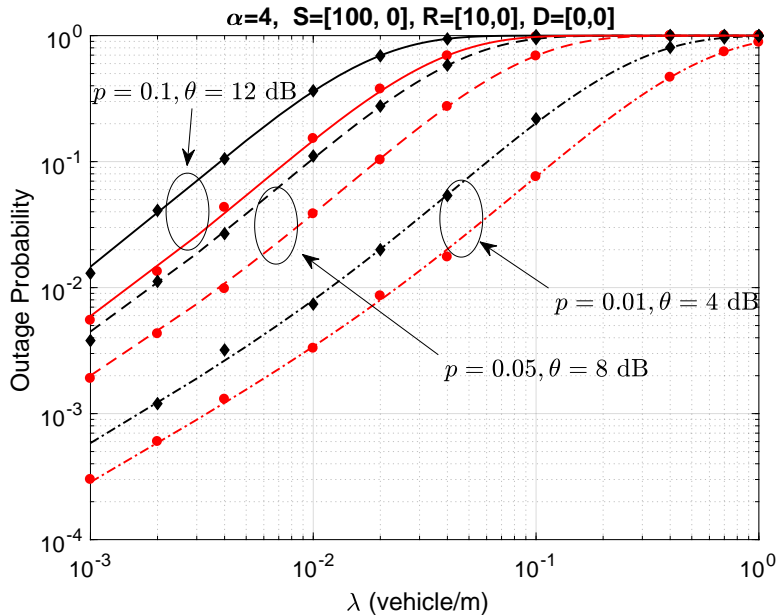


Fig. 8: Outage probability as function of  $\lambda$  for different values of  $p$  and  $\theta$  in a highway scenario (circle) and intersection scenario (diamond) considering MRC for the HSV model. Analytical results are plot with lines, and simulation results with marks.

3 relays in 200 meters or above, offer the same performance than using 7 relays or more. In Fig.7-b, we only plot the outage probability when using the relay  $R_1$ ,  $R_2$  and  $R_4$ . We can notice that the relay  $R_1$  covers the first  $[0,17 \text{ m}] \times [0,17 \text{ m}]$ , that is,  $289 \text{ m}^2$  ( $300 \text{ m}^2$ ). The relay  $R_2$  cover approximately  $4600 \text{ m}^2$  ( $4611 \text{ m}^2$ ), and then the relay  $R_4$  cover the rest, that is, more than  $35000 \text{ m}^2$  ( $35389 \text{ m}^2$ ).

The Fig. 8 compares the outage probability of a cooperative highway scenario with a single lane [16] and a cooperative intersection scenario with two orthogonal lanes. We can see from Fig. 8 that the outage probability increases as  $\lambda$ ,  $p$  and  $\theta$  increase (see Fig.3). One can notice that the highway scenario outperforms the intersection scenario in terms of outage probability. Intuitively, this is due to the fact that the intersection scenario has an additional lane that contributes to the aggregate of interference, therefore increasing the outage probability. We will see in the next figure the difference between the two scenarios.

In Fig. 9, we present the results for several values of  $r_{SD}$ , the relay is equidistant from the source and the destination. Without loss of generality, we set the triplet  $\{S, R, D\}$  on the same road. We plot the outage probability as a function of the distance from the intersection for  $r_{SD} \in \{50 \text{ m}, 150 \text{ m}, 250 \text{ m}\}$ . As for the results in Fig. 8, the highway scenario offers a better

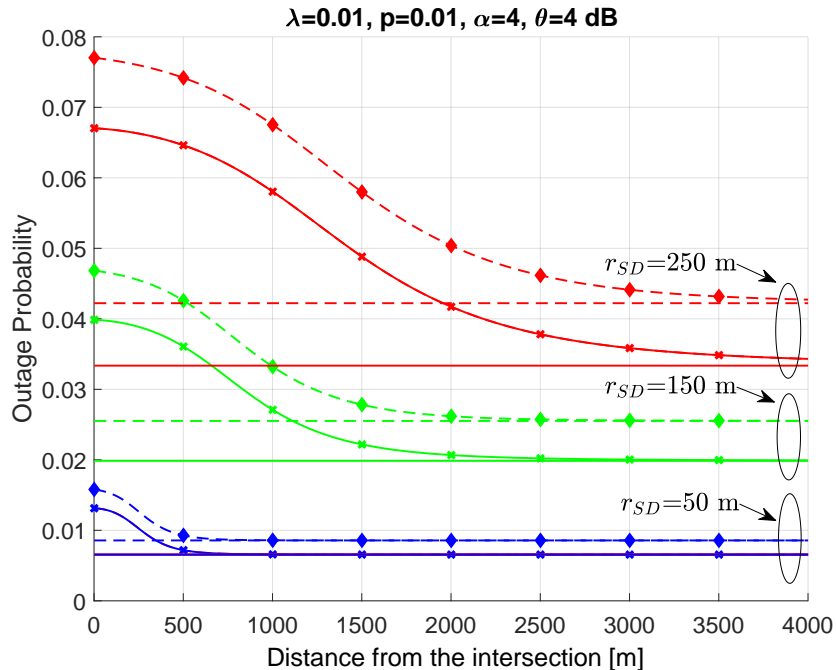


Fig. 9: Outage probability when varying the distance of the triplet  $\{S, R, D\}$  from the intersection for different values of  $r_{SD}$ . The highway scenario (line without marks) and the intersection scenario (line with marks) are considered, for the HSV model (simple line) and the LSV model (dashed line).

performance in terms of outage probability than the intersection scenario. But, as we increase the distance between the triplet and the intersection, the highway scenario and the intersection scenario converge toward the same value. This can be explained by the fact that, as vehicles move away from the intersection, the power of the interference originated from the other road becomes negligible, thus leading to the same performance as in a highway scenario. This further confirms the statement that the intersection scenario has a higher outage probability compared to the highway scenario, thus making intersections more critical areas because they are more prone to outage.

From Fig. 10, we see that, as  $\alpha$  increases, the outage probability decreases, this is intuitive, since the path loss function decreases faster for larger value of  $\alpha$ , thus leading to the rapid decrease of the interference power. We also see that, in a high traffic load ( $\lambda = 0.2$ ), the LSV model exhibits better performance. Inversely, in low traffic load, the HSV model exhibits a better performance. This confirms the results in Fig.2, Fig.3 and Fig.6. We note that for a low traffic scenario ( $\lambda = 0.03, \lambda = 0.05$ ), the gap in terms of outage probability between the LSV model

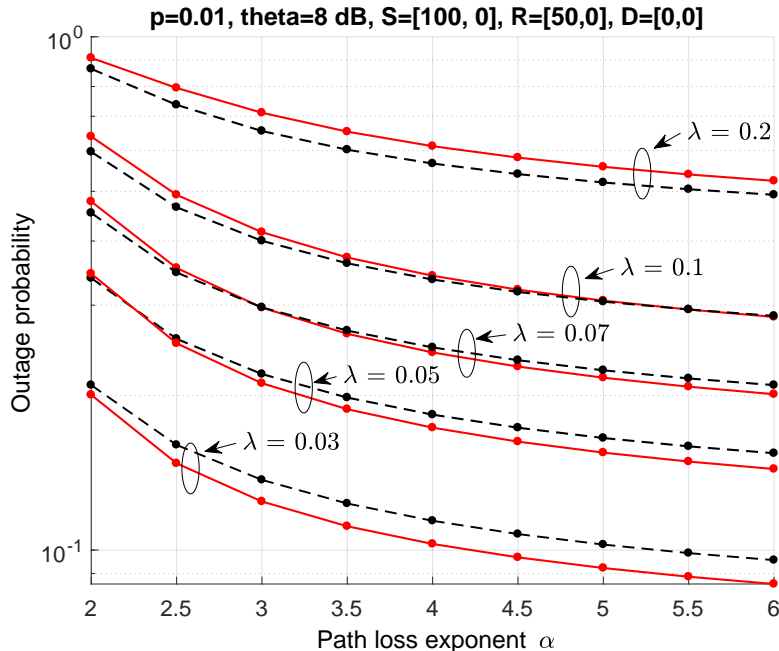


Fig. 10: Outage probability as a function of the path loss exponent  $\alpha$  for  $\lambda \in \{0.03, 0.05, 0.07, 0.1, 0.2\}$ , for the HSV model (line) and the LSV model (dashed line) considering MRC.

and the HSV model, for  $\alpha = 2$ , is very small, but, as  $\alpha$  increases, the gap becomes larger. Also, for  $\lambda = 0.07$ , the HSV model has a slightly higher value of outage probability than the LSV model when  $\alpha = 2$ , but, as the value of  $\alpha$  increases, the LSV model has a slightly high value of outage probability over the HSV model.

We conclude that larger values of  $\alpha$  lead to higher interference dependence, because the interference is dominated by vehicles that are close to the receiving nodes. On the opposite, lower values of  $\alpha$  lead to lower interference dependence, because the interference is a summation of several far vehicle signals which, to some extent, decreases the dependence of the interference [5]. Note that the path loss exponent  $\alpha$  depends on the environment. For instance,  $\alpha = 2$  corresponds to the free space,  $\alpha \in \{2.7, 3.5\}$  to an urban area, and  $\alpha \in \{3, 5\}$  to a shadowed urban area [26]. We can state that the environment plays an important role in the interference dependence. Indeed, an intersection in a suburban area has a lower dependence of interference, whereas an intersection in an urban has a higher interference dependence.

## VI. CONCLUSION

In this paper, we studied the performance of direct transmissions and cooperative transmissions for vehicular networks at road intersections in the presence of interference. We presented analytical results for two mobility models. Closed-form expressions were obtained for specific channel conditions. We also considered two decoding strategies: SC and MRC. We derive Laplace transform expressions when the receiving node can be anywhere on the plan, given finite and infinite road segments.

We showed that cooperative transmissions always enhance the performance compared to direct transmissions, and the use of MRC is only useful when the relay is closer to the source. We also showed that mobility increases the outage probability performance in good traffic conditions, whereas static or low mobility increases the outage probability performance in harsh traffic conditions. We also showed that the best relay position for the HSV model in low traffic conditions is when relay is closer to the destination. The best relay position for the HSV model in high traffic conditions is when relay is slightly shifted from the middle toward the destination. However, the best relay position in the LSV model is when the relay is equidistant from the source and the destination regardless of the traffic conditions. We showed that the outage probability does not improve after using 3 infrastructure relays.

We also showed that lower values of the path loss exponent leads to higher interference dependence. Finally, we showed that cooperative transmissions at intersections have higher outage probability than cooperative transmissions on highways.

As future works, we plan to analyze other medium access protocols, such as CSMA. We also plan to consider other channel models and other roads geometries.

## APPENDIX A

We calculate the first probability in equation (19)

$$\begin{aligned}
& \mathbb{P}(\mathcal{O}_{SR} \cap \mathcal{O}_{SD}^C) \\
&= \mathbb{E}_{I_X, I_Y} \left[ \mathbb{P} \left\{ \left( \frac{1}{2} \log_2 \left[ 1 + \frac{P|h_{SR}|^2 l_{SR}}{\sigma^2 + I_{X_R} + I_{Y_R}} \right] < R, \frac{1}{2} \log_2 \left[ 1 + \frac{P|h_{SD}|^2 l_{SD}}{\sigma^2 + I_{X_D} + I_{Y_D}} \right] \geq R \right) \right\} \right] \\
&= \mathbb{E}_{I_X, I_Y} \left[ \mathbb{P} \left\{ \left( |h_{SR}|^2 < \frac{\theta}{Pl_{SR}} (\sigma^2 + I_{X_R} + I_{Y_R}), |h_{SD}|^2 \geq \frac{\theta}{Pl_{SD}} (\sigma^2 + I_{X_R} + I_{Y_R}) \right) \right\} \right].
\end{aligned}$$



Since  $|h_{SR}|^2$  and  $|h_{RD}|^2$  both follow an exponential distribution with unit mean, we get

$$\begin{aligned}
\mathbb{P}(\mathcal{O}_{SR} \cap \mathcal{O}_{SD}^C) &= \mathbb{E}_{I_X, I_Y} \left[ 1 - \exp\left(-\frac{\theta}{Pl_{SR}} I_{X_R}\right) \exp\left(-\frac{\theta}{Pl_{SR}} I_{Y_R}\right) \exp\left(-\frac{\theta}{Pl_{SR}} \sigma^2\right) \right. \\
&\quad \left. \left( \exp\left(-\frac{\theta}{Pl_{SD}} I_{X_D}\right) \exp\left(-\frac{\theta}{Pl_{SD}} I_{Y_D}\right) \exp\left(-\frac{\theta}{Pl_{SD}} \sigma^2\right) \right) \right] \\
&= \mathbb{E}_{I_X, I_Y} \left[ \left( 1 - \exp(-K_{SR} I_{X_R}) \exp(-K_{SR} I_{Y_R}) \exp(-K_{SR} \sigma^2) \right) \right. \\
&\quad \left. \exp(-K_{SD} I_{X_D}) \exp(-K_{SD} I_{Y_D}) \exp(-K_{SD} \sigma^2) \right] \\
&= \mathbb{E}_{I_X, I_Y} [N_{SD} \exp(-K_{SD} I_{X_D}) \exp(-K_{SD} I_{Y_D}) \\
&\quad - N_{SR} \exp(-K_{SR} I_{X_R}) \exp(-K_{SR} I_{Y_R}) N_{SD} \exp(-K_{SD} I_{X_D}) \exp(-K_{SD} I_{Y_D})].
\end{aligned}$$

Given that the noise is independent of the interference, and using the independence of the PPP on the road  $X$  and  $Y$ , we finally get (21).

## APPENDIX B

To calculate the second probability in equation (19), we follow the same steps as in the Appendix A, and we obtain (22)

$$\begin{aligned}
\mathbb{P}(\mathcal{O}_{SR}^C \cap \mathcal{O}_{RD}^C) &= \\
&\mathbb{E}_{I_X, I_Y} \left[ \mathbb{P} \left\{ \left( |h_{SR}|^2 \geq \frac{\theta}{Pl_{SR}} (\sigma^2 + I_{X_R} + I_{Y_R}), |h_{RD}|^2 \geq \frac{\theta}{Pl_{RD}} (\sigma^2 + I_{X_D} + I_{Y_D}) \right) \right\} \right] \\
&= N_{SR} N_{RD} \mathbb{E}_{I_X} [\exp(-K_{SR} I_{X_R} - K_{RD} I_{X_D})] \mathbb{E}_{I_Y} [\exp(-K_{SR} I_{Y_R} - K_{RD} I_{Y_D})].
\end{aligned}$$

## APPENDIX C

To calculate the second probability in (20), we follow the same steps as in Appendix A, then we obtain:

$$\begin{aligned}
\mathbb{P}(\mathcal{O}_{SR}^C \cap \mathcal{O}_{SRD}^C) &= \mathbb{E}_{I_X, I_Y} \left[ N_{SR} \exp(-K_{SR} I_{X_R}) \exp(-K_{SR} I_{Y_R}) \right. \\
&\quad \left. \mathbb{P} \left\{ |h_{RD}|^2 l_{RD} + |h_{SD}|^2 l_{SD} \geq \frac{\theta}{P} (\sigma^2 + I_{X_D} + I_{Y_D}) \right\} \right]. \quad (44)
\end{aligned}$$

We write the probability inside the expectation in (44) as:

$$\mathbb{P}(\delta \geq \beta[\sigma^2 + I_{X_D} + I_{Y_D}] ),$$

where  $\delta = |h_{RD}|^2 l_{RD} + |h_{SD}|^2 l_{SD}$  and  $\beta = \theta/P$ .

The complementary cumulative distribution function of  $\delta$ , denoted  $\bar{F}_\delta(\cdot)$ , is given by:

$$\bar{F}_\delta(u) = \frac{l_{RD}e^{-u/l_{RD}} - l_{SD}e^{-u/l_{SD}}}{l_{RD} - l_{SD}}.$$

Then

$$\begin{aligned} \mathbb{P}(\delta \geq \beta[\sigma^2 + I_{X_D} + I_{Y_D}]) &= \\ &= \frac{l_{RD} \exp\left(-\frac{\beta}{l_{RD}}[\sigma^2 + I_{X_D} + I_{Y_D}]\right) - l_{SD} \exp\left(-\frac{\beta}{l_{SD}}[\sigma^2 + I_{X_D} + I_{Y_D}]\right)}{l_{RD} - l_{SD}}, \end{aligned} \quad (45)$$

plugging (45) into (44), and with some algebraic manipulations, we get (23).

## APPENDIX D

### PROOF OF THEOREM 1

When the interference at the relay and the destination are generated from two independent sets, the following expectation can be written as

$$\mathbb{E}_{I_X} [e^{-(sI_{X_R} + bI_{X_D})}] = \mathbb{E}_{I_X} [e^{-sI_{X_R}}] \mathbb{E}_{I_X} [e^{-bI_{X_D}}]. \quad (46)$$

Given that  $\mathbb{E}[e^{sI}] = \mathcal{L}_I(s)$ , we then develop the expression of the first expectation in (46)

$$\mathcal{L}_{I_{X_R}}(s) = \mathbb{E}[\exp(-sI_{X_R})]. \quad (47)$$

Plugging (1) into (47) yields

$$\begin{aligned} \mathcal{L}_{I_{X_R}}(s) &= \mathbb{E} \left[ \exp \left( - \sum_{x \in \Phi_{X_R}} sP|h_{Rx}|^2 l_{Rx} \mathbb{1}\{x \in \Phi_{X_R}\} \right) \right] \\ &= \mathbb{E} \left[ \prod_{x \in \Phi_{X_R}} \exp \left( - sP|h_{Rx}|^2 l_{Rx} \mathbb{1}\{x \in \Phi_{X_R}\} \right) \right] \\ &\stackrel{(a)}{=} \mathbb{E} \left[ \prod_{x \in \Phi_{X_R}} \mathbb{E}_{|h_{Rx}|^2} \left\{ \exp \left( - sP|h_{Rx}|^2 l_{Rx} \mathbb{1}\{x \in \Phi_{X_R}\} \right) \right\} \right] \\ &\stackrel{(b)}{=} \mathbb{E} \left[ \prod_{x \in \Phi_{X_R}} \frac{p}{1 + sPl_{Rx}} + 1 - p \right] \end{aligned}$$

$$\begin{aligned}
&\stackrel{(c)}{=} \exp \left( -\lambda_X \int_{\mathcal{B}} \left[ 1 - \left( \frac{p}{1 + sPl_{Rx}} + 1 - p \right) \right] dx \right) \\
&= \exp \left( -p\lambda_X \int_{\mathcal{B}} \frac{1}{1 + 1/sPl_{Rx}} dx \right),
\end{aligned}$$

where (a) follows from having independent fading; (b) follows from calculating the expectation over  $|h_{Rx}|^2$  which follows an exponential distribution with unit mean, and then calculating the expectation over the indicator function  $\mathbb{1}$ ; (c) follows from the probability generating functional (PGFL) of a PPP [27]. Then the right side of the equality in (46) can be expressed as

$$\mathbb{E}_{I_X} [e^{-sI_{X_R}}] \mathbb{E}_{I_X} [e^{-bI_{X_D}}] = \mathcal{L}_{I_{X_R}}(s) \mathcal{L}_{I_{X_D}}(b), \quad (48)$$

where:

$$\mathcal{L}_{I_{X_R}}(s) = \exp \left( -p\lambda_X \int_{\mathcal{B}} \frac{1}{1 + (A\|x - R\|^\alpha)/sP} dx \right) \quad (49)$$

$$\mathcal{L}_{I_{X_D}}(s) = \exp \left( -p\lambda_X \int_{\mathcal{B}} \frac{1}{1 + (A\|x - D\|^\alpha)/sP} dx \right). \quad (50)$$

In the same way, when the interference originating from the Y road at the relay and the destination are generated from two independent sets, the following expectation can be written as

$$\mathbb{E}_{I_Y} [e^{-sI_{Y_R}}] \mathbb{E}_{I_Y} [e^{-bI_{Y_D}}] = \mathcal{L}_{I_{Y_R}}(s) \mathcal{L}_{I_{Y_D}}(b), \quad (51)$$

where

$$\mathcal{L}_{I_{Y_R}}(s) = \exp \left( -p\lambda_Y \int_{\mathcal{B}} \frac{1}{1 + (A\|y - R\|^\alpha)/sP} dy \right) \quad (52)$$

$$\mathcal{L}_{I_{Y_D}}(s) = \exp \left( -p\lambda_Y \int_{\mathcal{B}} \frac{1}{1 + (A\|y - D\|^\alpha)/sP} dy \right). \quad (53)$$

After substituting all the expressions of the expectation in (21), (22) and (23), we obtain (24), (25) and (26).

## APPENDIX E

### PROOF OF THEOREM 2

When the interference at the relay and the destination are generated from the same set, the equality in (46) and (51) does not hold true. Then, the expectation in left side of (46) will be expressed as

$$\mathbb{E}_{I_X} \left[ e^{-(sI_{X_R} + bI_{X_D})} \right] = \mathbb{E}_{I_X} \left[ \prod_{x \in \Phi_X} \mathbb{E}_{|h|^2} \left[ e^{-sP|h_{Rx}|^2 l_{Rx} \mathbb{1}\{x \in \Phi_{X_R}\} + bP|h_{Dx}|^2 l_{Dx} \mathbb{1}\{x \in \Phi_{X_D}\}} \right] \right]$$

$$\begin{aligned}
&= \mathbb{E}_{I_X} \left[ \prod_{x \in \Phi_X} \frac{p}{(1 + sPl_{Rx})(1 + bPl_{Dx})} + 1 - p \right] \\
&= \exp \left( -\lambda_X \int_{\mathcal{B}} 1 - \left[ \frac{p}{(1 + sPl_{Rx})(1 + bPl_{Dx})} + 1 - p \right] dx \right) \\
&= \exp \left( -p\lambda_X \int_{\mathcal{B}} \frac{sPl_{Rx}}{1 + sPl_{Rx}} + \frac{bPl_{Dx}}{1 + bPl_{Dx}} - \frac{sbP^2l_{Rx}l_{Dx}}{(1 + sPl_{Rx})(1 + bPl_{Dx})} dx \right) \\
&= \exp \left( -p\lambda_X \int_{\mathcal{B}} \frac{dx}{1 + 1/sPl_{Rx}} \right) \exp \left( -p\lambda_X \int_{\mathcal{B}} \frac{dx}{1 + 1/bPl_{Dx}} \right) \\
&\quad \exp \left( p\lambda_X \int_{\mathcal{B}} \frac{sbP^2l_{Rx}l_{Dx}}{(1 + sPl_{Rx})(1 + bPl_{Dx})} dx \right). \tag{54}
\end{aligned}$$

Then (54) can be written as

$$\mathbb{E}_{I_X} \left[ e^{-(sI_{X_R} + bI_{X_D})} \right] = \mathcal{L}_{I_{X_R}}(s) \mathcal{L}_{I_{X_D}}(b) \rho_X(s, b) = \mathcal{L}_{I_{X_R}, I_{X_D}}(s, b). \tag{55}$$

Following the same steps, we obtain the expectation in the left side of (50)

$$\mathbb{E}_{I_Y} \left[ e^{-(sI_{Y_R} + bI_{Y_D})} \right] = \mathcal{L}_{I_{Y_R}}(s) \mathcal{L}_{I_{Y_D}}(b) \rho_Y(s, b) = \mathcal{L}_{I_{Y_R}, I_{Y_D}}(s, b). \tag{56}$$

After substituting all the expressions of the expectation in (21), (22) and (23), we obtain (27), (28), and (29).

## APPENDIX F

### PROOF OF PROPOSITION 1

In order to calculate the Laplace transform of interference originated from the X road at the relay, we have to calculate the integral in (34). We calculate the integral in (34) for  $\mathcal{B} = \mathbb{R}$  and  $\alpha = 2$ . Let us take  $k = sP/A^2$ ,  $n_x = n \cos(\theta_N)$  and  $n_y = n \sin(\theta_N)$ , then (34) becomes

$$\mathcal{L}_{I_{X_N}}(s) = \exp \left( -p\lambda_X k \int_{\mathbb{R}} \frac{1}{k + n_y^2 + (x - n_x)^2} dx \right), \tag{57}$$

and the integral inside the exponential in (57) equals

$$\int_{\mathbb{R}} \frac{1}{k + n_y^2 + (x - n_x)^2} dx = \frac{\pi}{\sqrt{n_y^2 + k}}. \tag{58}$$

Then, plugging (58) into (57) we obtain

$$\mathcal{L}_{I_{X_N}}(s) = \exp \left( -p\lambda_X k \frac{\pi}{\sqrt{n_y^2 + k}} \right). \tag{59}$$

Finally, substituting  $k$  and  $n_y$  in (59) yields (38). Following the same steps above, and without details for the derivation, we obtain (39).

## APPENDIX G

## PROOF OF PROPOSITION 2

We calculate the integral in (34) for  $\mathcal{B} = [-Z, Z]$  and  $\alpha = 2$ . We use the same change of variables as in **Proposition 1**, then we get

$$\begin{aligned} & \int_{-Z}^{+Z} \frac{1}{1 + (A\|x - N\|^2)/sP} dx = \int_{-Z}^{+Z} \frac{1}{1 + n_y^2 + (x - n_x)^2/k} \\ & = \int_{-Z}^{+Z} 1 - \frac{n_y^2 + (x - n_x)^2/k}{1 + n_y^2 + (x - n_x)^2/k} = 2Z - \int_{-Z}^{+Z} \frac{n_y^2 + (x - n_x)^2}{k + n_y^2 + (x - n_x)^2}. \end{aligned} \quad (60)$$

The integral in the last equality in (60) equals

$$\int_{-Z}^{+Z} \frac{n_y^2 + (x - n_x)^2}{k + n_y^2 + (x - n_x)^2} = \frac{2Z\sqrt{n_y^2 + k} - k \arctan\left(\frac{Z + n_x}{\sqrt{n_y^2 + k}}\right) - k \arctan\left(\frac{Z - n_x}{\sqrt{n_y^2 + k}}\right)}{\sqrt{n_y^2 + k}}, \quad (61)$$

then plugging (61) into (60) yields (40). Following the same steps above, we obtain (41).

## REFERENCES

- [1] U.S. Dept. of Transportation, National Highway Traffic Safety Administration, “Traffic safety facts 2015,” Jan. 2017.
- [2] M. Haenggi, R. K. Ganti *et al.*, “Interference in large wireless networks,” *Foundations and Trends® in Networking*, vol. 3, no. 2, pp. 127–248, 2009.
- [3] R. K. Ganti and M. Haenggi, “Spatial and temporal correlation of the interference in aloha ad hoc networks,” *IEEE Communications Letters*, vol. 13, no. 9, 2009.
- [4] R. Tanbourgi, H. Jäkel, and F. K. Jondral, “Cooperative relaying in a poisson field of interferers: A diversity order analysis,” in *Information Theory Proceedings (ISIT), 2013 IEEE International Symposium on*. IEEE, 2013, pp. 3100–3104.
- [5] M. Haenggi, “Diversity loss due to interference correlation,” *IEEE Communications Letters*, vol. 16, no. 10, pp. 1600–1603, 2012.
- [6] —, “Outage, local throughput, and capacity of random wireless networks,” *IEEE Transactions on Wireless Communications*, vol. 8, no. 8, 2009.
- [7] U. Schilcher, C. Bettstetter, and G. Brandner, “Temporal correlation of interference in wireless networks with rayleigh block fading,” *IEEE Transactions on Mobile Computing*, vol. 11, no. 12, pp. 2109–2120, 2012.
- [8] R. Tanbourgi, H. S. Dhillon, J. G. Andrews, and F. K. Jondral, “Effect of spatial interference correlation on the performance of maximum ratio combining,” *IEEE Transactions on Wireless Communications*, vol. 13, no. 6, pp. 3307–3316, 2014.
- [9] —, “Dual-branch mrc receivers under spatial interference correlation and nakagami fading,” *IEEE Transactions on Communications*, vol. 62, no. 6, pp. 1830–1844, 2014.
- [10] S. S. Ikki, P. Ubaidulla, and S. Aïssa, “Regenerative cooperative diversity networks with co-channel interference: Performance analysis and optimal energy allocation,” *IEEE Transactions on Vehicular Technology*, vol. 62, no. 2, pp. 896–902, 2013.

- [11] U. Schilcher, S. Toumpis, A. Crismani, G. Brandner, and C. Bettstetter, “How does interference dynamics influence packet delivery in cooperative relaying?” in *Proceedings of the 16th ACM international conference on Modeling, analysis & simulation of wireless and mobile systems*. ACM, 2013, pp. 347–354.
- [12] A. Crismani, S. Toumpis, U. Schilcher, G. Brandner, and C. Bettstetter, “Cooperative relaying under spatially and temporally correlated interference,” *IEEE Transactions on Vehicular Technology*, vol. 64, no. 10, pp. 4655–4669, 2015.
- [13] B. Błaszczyszyn, P. Muhlethaler, and Y. Toor, “Performance of mac protocols in linear vanets under different attenuation and fading conditions,” in *Intelligent Transportation Systems, 2009. ITSC’09. 12th International IEEE Conference on*. IEEE, 2009, pp. 1–6.
- [14] B. Błaszczyszyn, P. Muhlethaler, and Y. Toor, “Stochastic analysis of aloha in vehicular ad hoc networks,” *Annals of telecommunications-Annales des télécommunications*, vol. 68, no. 1-2, pp. 95–106, 2013.
- [15] B. Błaszczyszyn, P. Muhlethaler, and N. Achir, “Vehicular ad-hoc networks using slotted aloha: point-to-point, emergency and broadcast communications,” in *Wireless Days (WD), 2012 IFIP*. IEEE, 2012, pp. 1–6.
- [16] M. J. Farooq, H. ElSawy, and M.-S. Alouini, “A stochastic geometry model for multi-hop highway vehicular communication,” *IEEE Transactions on Wireless Communications*, vol. 15, no. 3, pp. 2276–2291, 2016.
- [17] Z. Tong, H. Lu, M. Haenggi, and C. Poellabauer, “A stochastic geometry approach to the modeling of dsrc for vehicular safety communication,” *IEEE Transactions on Intelligent Transportation Systems*, vol. 17, no. 5, pp. 1448–1458, 2016.
- [18] C. Jiang, H. Zhang, Z. Han, Y. Ren, V. C. Leung, and L. Hanzo, “Information-sharing outage-probability analysis of vehicular networks,” *IEEE Transactions on Vehicular Technology*, vol. 65, no. 12, pp. 9479–9492, 2016.
- [19] A. Tassi, M. Egan, R. J. Piechocki, and A. Nix, “Modeling and design of millimeter-wave networks for highway vehicular communication,” *IEEE Transactions on Vehicular Technology*, vol. 66, no. 12, pp. 10676–10691, 2017.
- [20] A. Al-Hourani, R. J. Evans, S. Kandeepan, B. Moran, and H. Eltom, “Stochastic geometry methods for modeling automotive radar interference,” *IEEE Transactions on Intelligent Transportation Systems*, vol. 19, no. 2, pp. 333–344, 2018.
- [21] E. Steinmetz, M. Wildemeersch, T. Q. Quek, and H. Wymeersch, “A stochastic geometry model for vehicular communication near intersections,” in *Globecom Workshops (GC Wkshps), 2015 IEEE*. IEEE, 2015, pp. 1–6.
- [22] M. Abdulla, E. Steinmetz, and H. Wymeersch, “Vehicle-to-vehicle communications with urban intersection path loss models,” in *Globecom Workshops (GC Wkshps), 2016 IEEE*. IEEE, 2016, pp. 1–6.
- [23] M. Abdulla and H. Wymeersch, “Fine-grained reliability for v2v communications around suburban and urban intersections,” *arXiv preprint arXiv:1706.10011*, 2017.
- [24] J. P. Jeyaraj and M. Haenggi, “Reliability analysis of v2v communications on orthogonal street systems,” in *GLOBECOM 2017-2017 IEEE Global Communications Conference*. IEEE, 2017, pp. 1–6.
- [25] T. Kimura and H. Saito, “Theoretical interference analysis of inter-vehicular communication at intersection with power control,” *Computer Communications*, 2017.
- [26] T. S. Rappaport, “Wireless communications—principles and practice, (the book end),” *Microwave Journal*, vol. 45, no. 12, pp. 128–129, 2002.
- [27] M. Haenggi, *Stochastic geometry for wireless networks*. Cambridge University Press, 2012.